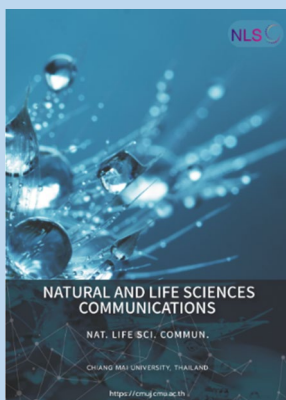


Research article

**Editor:**

Sirasit Srinuanpan,
Chiang Mai University, Thailand

Article history:

Received: August 3, 2023;
Revised: February 3, 2024;
Accepted: February 13, 2024;
Published online: February 20, 2024
<https://doi.org/10.12982/NLSC.2024.019>

Corresponding author:

Nanik Purwanti,
E-mail: nanik_purwanti@apps.ipb.ac.id



Open Access Copyright: ©2024 Author (s). This is an open access article distributed under the term of the Creative Commons Attribution 4.0 International License, which permits use, sharing, adaptation, distribution, and reproduction in any medium or format, as long as you give appropriate credit to the original author (s) and the source.

Response Surface Methodology for Optimization of Mucilage Extraction from *Dioscorea alata* Tuber

Dewi Fortuna¹, Emmy Darmawati², Titi Candra Sunarti²,
Sutrisno Suro Mardjan², Siti Mariana Widayanti³,
Nancy Dewi Yuliana², and Nanik Purwanti^{2,*}

¹ Agricultural Engineering Science, IPB University, P. O. BOX 220, Bogor 16002, Indonesia.

² IPB University, P. O. BOX 220, Bogor 16002, Indonesia.

³ Research Centre for Agroindustry, National Research and Innovation Agency, Jl. Raya Jakarta-Bogor, Cibinong, Bogor 16915, Indonesia.

ABSTRACT

Dioscorea alata mucilage (DAM) is a water-soluble polysaccharide and is composed of glucomannan. In this research, mucilages from *D. alata* were extracted using Response surface methodology (RSM) with a Central Composite Design (CCD) followed by distance-based optimality design, with three independent variables applied, i.e., temperature (4 – 60°C), time (0 – 30 h), and centrifugal speed (1.386 – 22.615×g). The maximum DAM yield was 5.89% ± 0.50%, which was obtained with an extraction temperature of 36.2°C for 13.3 h extraction time and centrifugation at 12,322×g. The regression model from RSM – CCD predicted that the maximum DAM yield was 5.47%, with R² of 99.59% and adjusted R² of 97.72%, which shows a significant correlation between the experimental and predicted values. The DAM is a complex material that mainly contains polysaccharides, i.e., β-pyranose forms of glucose and mannose, with low protein content. Water and oil holding capacity of the DAM powder were 8.43 g/g and 5.08 g/g, respectively, which considered as the highest compared to other similar studies.

Keywords: *Dioscorea alata* mucilage, Extraction, Optimization, Response surface methodology, Physicochemical properties

Funding: The authors are grateful for the research funding provided by the Beasiswa Unggulan Dosen Indonesia Dalam Negeri (BUDIDN) Program, Ministry of Education and Culture of the Republic of Indonesia; and The Indonesia Endowment Fund for Education (LPDP), Ministry of Finance of the Republic of Indonesia.

Citation: Fortuna, D., Darmawati, E., Sunarti, T.C., Mardjan, S.S., Widayanti, S.M., Yuliana, N.D., and Purwanti, N. 2024. Response surface methodology for optimization of mucilage extraction from *Dioscorea alata* tuber. Natural and Life Sciences Communications. 23(2): e2024019.

INTRODUCTION

Dioscorea alata (*D. alata*) is a staple food in Southeast Asia and Africa. (Garedew et al., 2017; Maneenoon et al., 2008) that contains a variety of nutritional and chemical ingredients, such as polysaccharides, proteins, polyphenols, flavonoids, saponins and diosgenin (Lebot et al., 2018; Narkhede et al., 2013), which some of those were identified in the mucilage (Alves et al., 2002; Fortuna et al., 2020). Recent studies reported that the mucilage extracted from *Dioscorea* sp. has natural antioxidant properties (Zhi et al., 2019), antimutagenic activity (Zhang et al., 2016), anti-inflammatory activity (Li et al., 2016) and antitumor activity (Liu et al., 2016). The mucilage comprises mostly water-soluble polysaccharides, in which the main monosaccharides composition are glucose (49.50%), galactose (10.90%), and mannose (33.40%) (Ma et al., 2017a; Zhi et al., 2019). The mucilage of *Dioscorea* sp. is potential for various food applications such as a food thickener (Ma et al., 2017b), a stabilizer (Lozano et al., 2022), an edible film (Wang et al., 2020; Li et al., 2021), a food binder and an emulsifier (Ma et al., 2020). Nevertheless, the yield of mucilage extraction from *Dioscorea* sp. turns to be a challenge for further utilization. The mucilage yield of various *Dioscorea* sp. was reported in the range of 1.58 – 8.00% (Nagai et al., 2014; Ma et al., 2017c; Zhi et al., 2019; Fortuna et al., 2020), which is considered as low.

Solvent extraction is commonly used to extract mucilage from *Dioscorea* sp. (Misaki et al., 1972; Fu et al., 2004; Hong-rui et al., 2010; Huang et al., 2020; Lozano et al., 2022), the solid sample is immersed in the solvent, and the extract is collected after the equilibrium extraction is reached (Chan et al., 2014). Solvent extraction is a widely employed method in plant extraction procedures because it can facilitate the extraction of pure and concentrated mucilage (Waghmare et al., 2022). According to Zhao et al. (2017), extraction of *Dioscorea hemsleyi* mucilage (DHM) using hot and warm water extraction (11.54 – 12.39%) with ethanol precipitation had the highest yield than ultrasound-assisted extraction (4.34%). Coldwater extraction with ethanol precipitation can be considered an effective and cost-effective technique to obtain high-quality mucilage with suitable industrial applications. In contrast, the ultrasonication method is more expensive but results in a higher amount of mucilage than other emerging techniques (Tosif et al., 2022). Furthermore, solvent extraction is employed to modernize traditional equipment, aligning it with the current demands of the market (Garcia-Vaquero et al., 2020).

Many factors affect extraction process of *D. alata* mucilage (DAM) such as extraction time, temperature, water to tuber ratio, pH, salt concentration and centrifugation (Berk, 2018; Fortuna et al., 2020; Hong-rui et al., 2010; Zhang and Wang, 2017). Mistry et al. (1992) stated that extraction must consider the maximum yield and the minimum use of energy and time. According to Huang et al. (2011), higher extraction temperature and longer time of extraction time will increase mass transfer rate of mucilage, hence its solubility. Extraction temperature affects the extraction rate, yield, molecular weight, mucilage activity, and starch gelatinization (Hong-rui et al. 2010; Zhao et al. 2017). The extraction rate and mucilage yield would decrease if the extraction temperature is above 70°C because *Dioscoreae* starch gelatinizes (Hong-rui et al., 2010). According to Zhao et al. (2017), hot water extraction (80°C, 90 minutes) of DHM produced a yield of 12.39% and a molecular weight of 1,004.2 kDa. These were higher than cold water extraction (25°C, 90 minutes) which resulted in a yield of 3.85% and a molecular weight of 36.5 kDa. The extraction time must be considered because the mucilage molecules need time to diffuse out of its matrix. According to Hong-rui et al. (2010), three hours extraction resulted in the highest yield, i.e., 14.6%; however, prolonged extraction time would increase the yield of dissolved starch. Huang et al. (2020) stated that high temperatures and long-time extraction would cause starch to gelatinize, thereby affecting extraction efficiency. Mucilage during

the extraction process usually traps small starch granules, and centrifugation is required to separate them. Centrifugation can break down soluble carbohydrate-protein complexes, and further separate starch and mucilage, whereas centrifugation speed can increase mucilage purity (Fu et al., 2004). Some studies that have been conducted to optimize extraction process of mucilage from *Dioscorea* sp. resulted in diverse process parameters and yields. According to Luo (2012), the optimum extraction of *Dioscorea nipponica* Makino mucilage with a water-tuber ratio of 33:1, extraction time of 134 minutes, and extraction temperature of 95°C produced a mucilage yield of 3.82%. Optimal conditions for mucilage extraction of *Dioscorea* sp. were at 100°C for 140 min at a water:tuber ratio of 3:1, which resulted in a maximum yield of 1.56% (Huang et al., 2011). Another research showed a maximum yield of 3.37% with extraction temperature of 40°C for 2h at pH 4.5 with 2% cellulose enzyme (Yuan-yuan et al., 2015). Hong-rui et al. (2010) showed that the use of water:tuber ratio of 8:1, pH 8.0, and extraction temperature of 60°C for 3 h increase the yield of mucilage to 15.1%.

Adopting the above-described studies for extracting mucilage from *D. alata* to obtain the optimum yield would make numerous combinations of experimental conditions to be tested, which are time-consuming and costly. Therefore, Response Surface Methodology (RSM) was considered in this research to minimize time and optimize cost. RSM is an optimization technique adopted to optimize several process and formulation variables and is systematically evaluated against influential process parameters and product quality (Saepang et al., 2024). RSM is often reported for optimizing extraction process of valuable compounds from agricultural produce, such as polysaccharide from *Dioscorea* sp. (Hong-rui et al., 2010; Zhang and Wang, 2017); protein from rice bran (Jongjareonrak et al., 2015); patchouli leaves oil (Kusuma and Mahfud, 2017); pectin from citrus peels (Chien et al., 2022); or bioactive extract from Napier grass (Thaisungnoen et al., 2024). RSM analyses multiple variables and their interactions with minimum number of experiments to obtain statistically acceptable results (Montgomery, 2013). Two common RSM approaches, central composite design (CCD) and Box Behnken Design (BBD), have been frequently utilized for the extraction optimization of mucilage (Luo, 2012; Han et al., 2016; L. Zhang and Wang, 2017; Bukhari et al., 2022). According to Stamenković et al., (2018), the CCD-RSM was recommended for optimization of solid-liquid extraction processes. Kusuma et al., (2015) stated modelling RSM from extraction parameters of natural dye from *Swietenia mahagoni* with microwave-assisted extraction method, which evaluated by CCD better prediction than BBD. These methods were statistically compared by root mean square error (RMSE) and absolute average deviation (AAD).

RSM-CCD was used due to its high flexibility and minimizing the waste of resources. The CCD has the axial points ($-\alpha$, α) as characteristic parameters. These points are beyond the minimum and maximum limits of the factors, guaranteeing the curvature of the response surface and enabling optimal conditions. The evaluation of the principal, interaction, and quadratic effects enables do independently, interpreting results easier (Leyva-Jiménez et al., 2022). This research proposed the application of RSM by employing CCD to optimize the extraction yield of DAM, using water-based extraction followed by alcohol precipitation (Fortuna et al., 2020). The objective of this research was to optimize DAM extraction using RSM and to investigate the physicochemical properties of the dried mucilage. The novelty of this research lies in the application of RSM to optimize extraction parameters of *D. alata* mucilage for achieving the maximum yield of extract and the functional properties of the optimized product.

Independent variables that were evaluated in this study were extraction temperature, extraction time and centrifugal speed of separation. We hypothesized that a model derived from RSM-CCD would be able to specify a relationship between the mucilage yield and the independent variables, whereas regression coefficients can describe the size (value) and direction of the relationship between an independent variable and the mucilage yield, either

positive or negative relationship. Mucilage structures and its physicochemical properties, obtained from the most optimum combination of variables applied in the extraction process, were also analysed.

MATERIAL AND METHODS

Materials

D. alata with yellow tuber was planted in the Research Farms in IPB University, East Java, Indonesia, and the tubers were harvested approximately 12 months after planting, and the moisture content was 70.86% db. All chemicals used in this study i.e., were ethanol absolute, CaCl_2 , $(\text{NH}_4)_2\text{SO}_4$, H_3BO_3 , Bromocresol green, H_2SO_4 , NaOH , SeO_2 , $\text{CuSO}_4 \cdot 5\text{H}_2\text{O}$, methyl red indicator, phenolphthalein, HCl were of analytical grades obtained from Merck, Germany. Corn oil was obtained from Nutrifood, Indonesia, and bi-distilled water were used for analysis.

Extraction of *D. alata* mucilage (DAM)

Extraction procedure of DAM followed the methods of our previous study (Fortuna et al., 2020) with few adaptations for optimization. Yield of DAM was expressed as a ratio between weight of DAM powder (m_{DAM}) to the weight of peeled tubers (m_{tp}), as shown in the following equation:

$$\text{DAM yield } \left(\% \frac{w}{w} \right) = \frac{m_{\text{DAM}} (g)}{m_{\text{tp}} (g)} \times 100 \quad (1)$$

Experimental design and statistical analysis

RSM using a CCD was used to optimize the effects of extraction temperatures, x_1 ; extraction times, x_2 , and centrifugal speeds, x_3 on DAM yield (Y). Table 1 presents the range of independent variables and their levels.

The whole design consisted of twenty experimental points in random order. The experimental data were fitted to a regression model, with the response function (Y) was the DAM yield (%) as shown in Equation (2).

$$Y = \beta_0 + \sum_{i=1}^3 \beta_i x_i + \sum_{i=1}^3 \beta_{ii} x_i^2 + \sum_{i=1}^2 \sum_{j+1}^3 \beta_{ij} x_i x_j + \varepsilon \quad (2)$$

Coefficients of the model were represented by β_0 as a constant coefficient, β_i as linear effects, β_{ii} as quadratic effects, and β_{ij} as interactions effects.

RSM was applied to the experimental data using Minitab (v. 17, Minitab LLC, USA). Response surface plots were also generated with the same software to visualize the effects of the individual and cumulative test variables on the response. An extra step by assigning distance-based optimality had to be performed to get model maximization if the RSM outcome was model minimization (Montgomery, 2013). Validation of the model was performed with experiments ($n=3$) using the optimal conditions indicated by the model that resulted in the maximum DAM yield.

Table 1. Response surface central composite design of the independent variables (actual and coded levels) for *D. alata* mucilage extraction.

Run	Independent variables					
	Actual level			Coded level		
	Extraction temperature x_1 (°C)	Extraction Time x_2 (h)	Centrifugal speed x_3 (×g)	Extraction temperature x_1 (°C)	Extraction time x_2 (h)	Centrifugal speed x_3 (×g)
1	49	6	5,500	+1	-1	-1
2	32	15	12,000	0	0	0
3	32	15	12,000	0	0	0
4	15	24	18,500	-1	+1	+1
5	15	6	5,500	-1	-1	-1
6	15	6	18,500	-1	-1	+1
7	49	24	5,500	+1	+1	-1
8	32	15	12,000	0	0	0
9	49	24	18,500	+1	+1	+1
10	32	15	12,000	0	0	0
11	49	6	18,500	+1	-1	+1
12	15	24	5,500	-1	+1	-1
13	60	15	12,000	+1.633	0	0
14	32	15	12,000	0	0	0
15	32	0	12,000	0	-1.633	0
16	32	15	22,615	0	0	+1.633
17	32	15	1,386	0	0	-1.633
18	32	30	12,000	0	+1.633	0
19	4	15	12,000	-1.633	0	0
20	32	15	12,000	0	0	0

Fourier Transform Infrared (FT-IR) analysis

Functional groups of DAM were analysed using a Fourier Transform Infrared (FT-IR) spectrophotometer (Alpha II, Bruker, Germany). The DAM powder was placed on the crystal of the attenuated total reflection (ATR) accessory. The spectra were recorded at the absorbance mode with a wavelength region from $4,000\text{ cm}^{-1}$ to 400 cm^{-1} .

Scanning Electron Microscopy (SEM)

Morphology of DAM powder was observed using FEI Quanta 650 environmental scanning electron microscope (ESEM) (FEI Company, Hillsboro, Oregon, USA). The scanning was operated in a slow vacuum mode at 60 Pa using a large field detector (LFD) at a voltage of 10 kV, and 10 mm distance. The images were captured at a magnification of 500× and 3,000×.

Physicochemical Properties

Whiteness index

Whiteness index was measured using a WSB-1 digital whiteness meter (Shanghai Jingke Scientific Instrument Co., Ltd., Shanghai, China). The result was expressed as a whiteness index.

pH

pH of DAM dispersion (10% w/w) was recorded by a hand-held pH meter D-51E (Horiba, Ltd, Kyoto, Japan).

Protein Content

Protein content was determined using Kjeldahl method using a nitrogen conversion factor of 6.5.

Water and oil holding capacity

Water holding capacity (WHC) of DAM powder was measured using a centrifugation method developed by Suzuki et al. (1996) with some adjustments. 200 mg of powder was placed in a centrifuge tube, to which 20 mL of bi-distilled water was added. The tubes were left in a shaking water bath for 24 h at room temperature to allow complete hydration of the powder. The fully hydrated powder was centrifuged at 2,500×g for 60 min after which the supernatant was carefully decanted, and the pellet was collected. The wet pellet was weighed (wet_p) prior to drying the pellet using an air dryer at 120°C for 2 h (dry_p). The WHC was calculated by the following equation:

$$WHC = \frac{wet_p(mg) - dry_p(mg)}{200\text{ mg}} \quad (3)$$

Oil holding capacity (OHC) was determined using a similar procedure as WHC determination. Two grams (m_d) of DAM was mixed with 20 mL of corn oil in a centrifuge tube. The mixture was vortexed for 10 s every 5 min for 30 min. The mixture was let to rest at room temperature ($30 \pm 2^\circ\text{C}$) for 30 min and then centrifuged at 2,500×g for 30 min. The supernatant was decanted, and the precipitate was collected. The precipitate was placed on a filter paper to remove excess oil prior to weighing (m_w). The OHC was calculated using Equation (4):

$$OHC = \frac{m_w(g) - m_d(g)}{m_d(g)} \quad (4)$$

Emulsion activity

Emulsion activity of the DAM powder was measured using the method of Yasumatsu et al. (1972) with some modifications. One gram of DAM powder was suspended in 12.5 mL bi-distilled water and then 12.5 mL of corn oil was added to it. The mixture was homogenized at 12,000 rpm for 1 min using WTW Disper D-8 (Xylem Analytics Germany Sales GmbH and Co. KG, Wilhelm, Germany). The emulsion was allowed to rest for 30 min after which two phases were observed, i.e., the emulsified layer at the top and water layer at the bottom. The emulsion activity (EA) was expressed as the percentage ratio between the height of emulsified layer (H_E) and the height of the whole layer in the centrifugal tube (H_T).

$$EA (\%) = \frac{H_E}{H_T} \times 100 \quad (5)$$

Statistical analysis

All analysis was performed in triplicate and the results were presented as the mean values and their standard deviations.

RESULTS

Model fitting and optimization

Effects of the process variables, i.e., extraction temperature (x_1), extraction time (x_2), and centrifugal speed (x_3) on the extraction yield obtained from the experiments were analysed through RSM-CCD. The model suggested that the optimal model to predict DAM yield using RSM-CCD gave a minimum response, whereas the optimization using RSM in this study aimed to maximize the yield. An extra step using distance-based optimality design was performed using Minitab software. The software generated selected design points to come up with the maximum responses. The selected design points consisted of twelve experimental-sets used for calculating the variance, which led to the following second-order polynomial equation.

$$Y = -6.63 + 0.2364x_1 + 0.4396x_2 + 0.000798x_3^* - 0.004140x_1x_1 - 0.01366x_2x_2 + 0.000704x_1x_2^* + 0.000004x_1x_3 + 0.000008x_2x_3 \quad (6)$$

Based on ANOVA, from which the summary is shown in Table 2, Equation (6) can be used to predict the experimental data designed in Table 1, with a high significance ($P < 0.05$). The F-value obtained indicates that the model can describe variations of the responses.

Table 2. Analysis of variance of the fitted model obtained from distance-based optimality design to maximize the DAM yield.

Sources	Degree of freedom	Sum of Squares	Mean of Squares	F-Value	P-Value
Model	9	3.72	0.41	53.48	0.018
Error	2	0.02	0.01		
Total	11	3.74			

Figure 1 represents the standardized Pareto chart for CCD for yield as response variables from the data of Table 1. A Pareto chart, which orders the factors according to their significance, the sequence of effective variables and their interactions for yield were $x_1 > x_2 > x_2x_3 > x_1x_3 > x_3x_3 > x_1x_1 > x_2x_2 > x_1x_2 > x_3$.

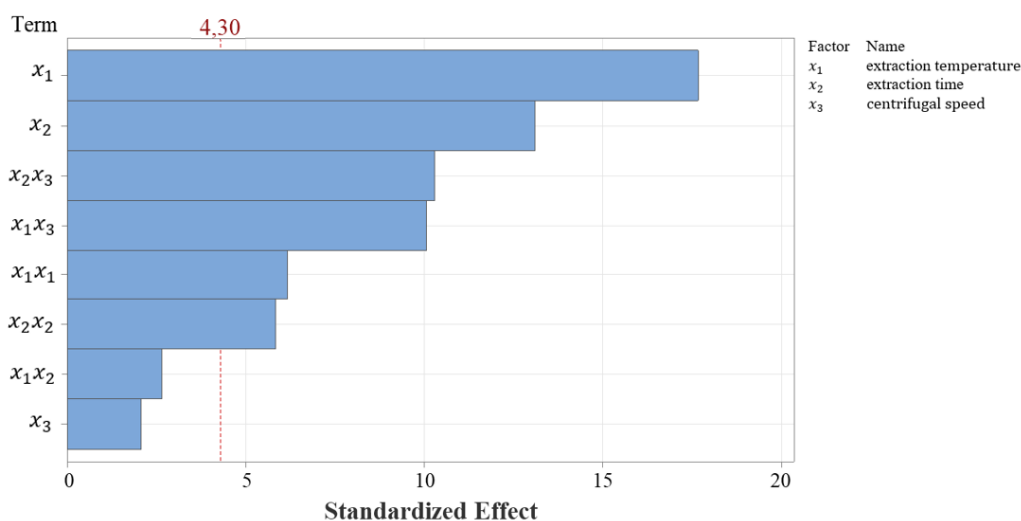


Figure 1. Pareto chart showing the order of significance of factors with yield as the response variable; $\alpha = 0.05$

Surface plot analysis of DAM yield

Graphical representations of the regression model that was summarized in Table 2 are depicted as surface plots (Figure 2A-C). Two independent variables were continuously set in the plots, whereas the other variable was kept constant at their respective centre of the test ranges. The constant variable was set as zero level in terms of coded factors. Through these plots, the optimal combination of the independent variables to maximize the response can be identified.

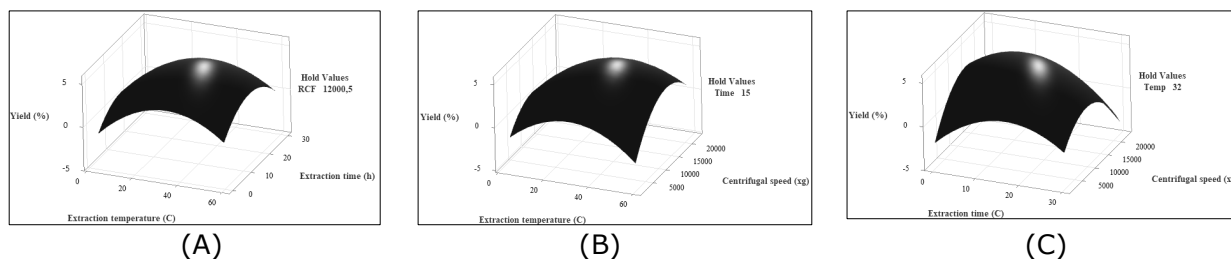


Figure 2. Surface plots of DAM yield as functions of extraction temperature, time, and centrifugal speed. (A) The effects of extraction temperature, °C, (x_1) and time (x_2) on the DAM yield (Y) with centrifugal speed (x_3) set at 12,000.5×g; (B) the effects of extraction temperature, °C, (x_1) and centrifugal speed (x_3) on the yield (Y) with extraction time (x_2) set at 15 h; (C) the effects of extraction time (x_2) and centrifugal speed (x_3) on the yield (Y) with extraction temperature (x_1) set at 32°C.

The 3D response surface plot showing the combined effect of extraction temperature (x_1) and time (x_2) on the yield of DAM at a constant centrifugal speed of 12,000.5 ×g is presented in Figure 2(A). As the extraction temperature and time increased, the yield of DAM also increased and reached a maximum of 5.461% at an extraction temperature of 35.48°C and an extraction time of 13.36 h. However, after these threshold values, the yield of DAM decreased to 4.51% at an extraction temperature of 50.96°C and an extraction time of 14.37 h.

The combined effect of extraction temperature (x_1) and centrifugal speed (x_3) on the yield of DAM is shown in Figure 2(B) at an extraction time (x_2) set at 15 h. The yield of DAM increased from 0.05 - 5.43% by increasing extraction temperature from 7.15 - 36.13°C and centrifugal speed from 2,621.93 - 12,089.5 ×g.

At a set extraction temperature (x_1) of 32°C, the effect of extraction time (x_2) and centrifugal speed (x_3) on the yield of DAM is shown in Figure 2(C). At an extraction time of 2.57 h and centrifugal speed of 2,806.56 ×g, the yield of DAM is meager, only 0.07%. However, by increasing extraction time and centrifugal speed, the DAM yield increased significantly and reached a maximum of 5.40% at extraction time 13.62 h and centrifugal speed 11,955.5 ×g.

Model validation

Based on the model obtained from the distance-based optimality design, experiments were performed with the optimal conditions set at 36.2°C, 13.3 h, and 12,322×g to validate the predicted response. Figure 3(A) illustrates ethanol separation of DAM in which DAM was located at the top layer and Figure 3(B) shows the top view of the DAM during ethanol separation.

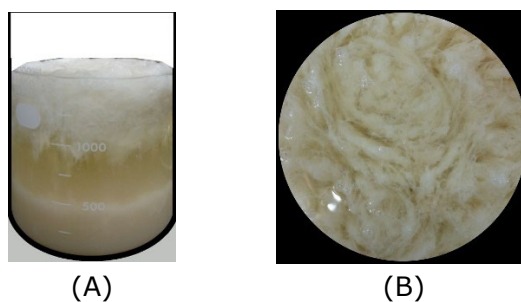


Figure 3. Ethanol separation of DAM in which DAM was located at the top layer (A) and the top vies of the DAM during ethanol separation (B).

The result showed that the maximum extraction yield for DAM was 5.89 ± 0.50 (%) ($n=3$), which closely agreed with the predicted response of the model, i.e., 5.47%. The validation showed insignificant difference between the experimental and predicted values. The DAM powder obtained from the optimal conditions, i.e., 36.2°C, 13.3 h, and 12,322×g, were further analyzed in terms of their structures and physicochemical properties as follows.

FTIR analysis

Figure 4 shows FTIR spectra of DAM powder with the main spectra observed at 3307, 2925, 1640, 1366, 1150, 1078, 1019, 933, 848, and 760 cm^{-1} .

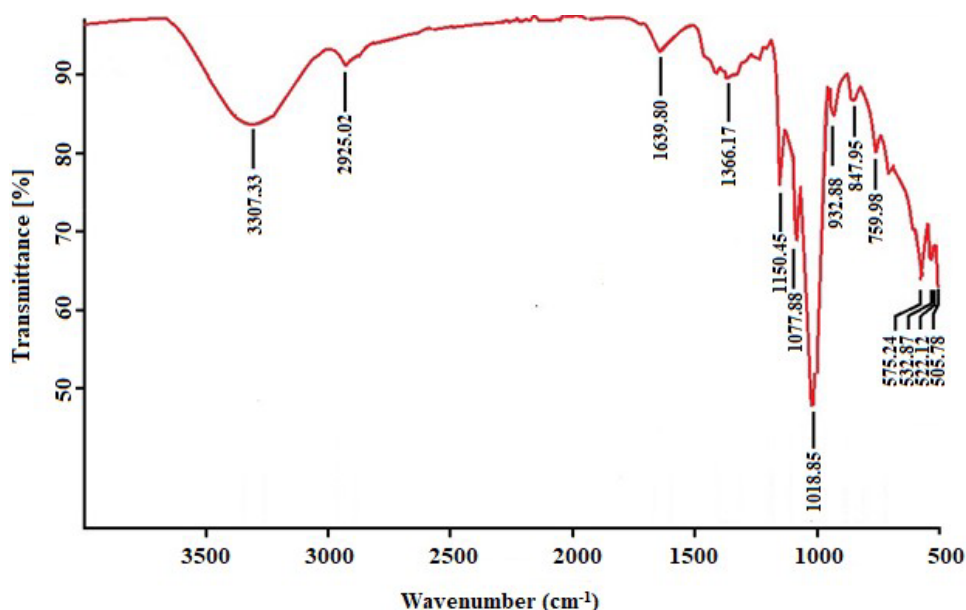


Figure 4. Fourier Transform infrared spectra of DAM powder, which shows some dominant functional groups.

SEM

Figure 5 shows morphology of DAM powder taken with SEM at magnification of 500x (A) and 3000x (B). The shape of DAM was irregular and rough with different sizes (~ 11.87 - 43.12 μm) and porosity.

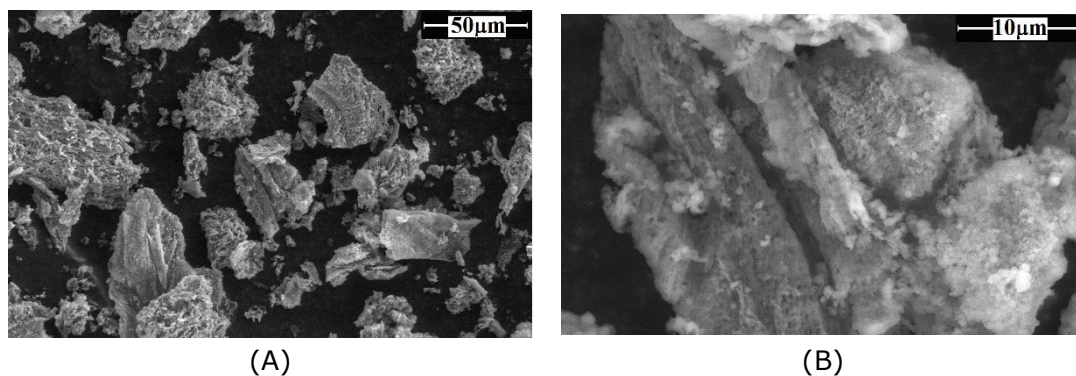


Figure 5. Scanning electron micrographs of microstructures DAM powder observed at magnification of (A) 500 \times and (B) 3000 \times .

Physicochemical properties

Whiteness index, pH, protein content, WHC, OHC, and EA of the DAM powder are summarized in Table 3.

Table 3. Physicochemical properties of DAM powder.

Physicochemical Properties	Values
Whiteness index	90.77 \pm 0.02
pH	6.70 \pm 0.01
Protein content (%)	0.37 \pm 0.57
WHC (g water/g sample)	8.43 \pm 0.32
OHC (g oil/g sample)	5.08 \pm 0.13
EA (%)	35.61 \pm 0.45

DISCUSSION

The optimum condition of DAM mucilage was successfully predicted using RSM-CCD followed by distance-based optimality design, which resulted in the second-order polynomial regression model (Equation 6). There are individual effects of each process variable, which are represented in the linear coefficients (x_1 , x_2 , and x_3), and the interactions between process variables, which are represented in the interaction coefficients (x_1x_2 , x_2x_3 , and x_1x_3). Equation (6) shows that the linear and interaction coefficients are positive, while the quadratic coefficients of x_1 and x_2 are negative. These mean that the higher DAM yield would be obtained if the independent variables with positive coefficients are increased. Nevertheless, the quadratic effects of the variables should also be considered because they cause reduction of the yield. In addition, the effects of centrifugal speed (x_3) and the interaction between temperature (x_1) and time (x_2) to the DAM yield are not significant as indicated by the asterisk sign. The ANOVA analysis of the model and the experimental data showed R^2 of 99.59%, which means that 99.59% of the total variations in the results were attributed to the variables investigated. The adj- R^2 was 97.72% that indicates high correlation between the experimental and predicted values. The standard deviation (SD) value of 0.088 indicates that the distance between the data values and the predicted values is small, which means the experimental response can be well-described by the model.

The surface plot depicted correlation between extraction temperature and time (Figure 2(A)) show that the DAM yield increased with the extraction temperature up to 50°C and time up to 20 h, beyond which the yield decreased. Decreasing the DAM yield with higher temperature than 50°C might be attributed by starch gelatinization, which makes the mucilage adheres to the starch granules. Gelatinization of *D. opposita* starch started to increase at 57.5°C and reached its peak at 67.7°C (Li et al., 2015). Short extraction time and high extraction temperature might be better to give desirable extraction yield (Luo, 2012). Centrifugal speed as a linear term exhibited a poor effect ($P > 0.05$) on the yield, but its interaction with extraction temperature had a significant synergistic effect ($P < 0.05$) (Figure 2(B)). Based on these two independent variables, the predicted maximum yield of DAM would be achieved when the extraction temperature is around 35°C and the centrifugal speed is around 6,000 μg . The surface plots depicted the correlation between extraction time and centrifugal speed (Figure 2(C)) show that the extraction time has a more positive effect on the DAM yield than the centrifugal speed. The mutual interaction between the extraction time and centrifugal speed would result in the maximum yield at around 15 h and 12,000 μg . Result of the model validation at the optimal conditions indicates that designing the experiments using RSM-CCD, and further deriving a model of optimization from the experimental results was proven to be an effective tool to maximize the DAM yield with a smaller number of experiments rather than trying all combinations of variables.

DAM powder, produced using the optimal conditions predicted by the model, is a complex material because the FTIR spectra (Figure 4) consist of more than five spectrum bands (Nandiyanto et al., 2019). The broad band at 3,307 cm^{-1} indicates the existence of hydroxyl group in the form of -hydrogen-bonded O-H stretch. Similar band was observed in konjac glucomannan with the band located at 3,391.59 cm^{-1} (Widjanarko et al., 2011). Bands in the range of 3,000 - 4,000 cm^{-1} are usually related to -OH oscillations in water molecules (Nawrocka et al., 2018). A small spectra is observed at 2,925 cm^{-1} , which represents CH stretching, and it may arise from methyl units (Hui et al., 2019). The remarkable feature of the DAM spectra is the presence of peaks correspond to the protein bands, i.e., 1639.80 cm^{-1} , which can be assigned to C=O stretch vibration and 1366.17 cm^{-1} , which can be assigned to asymmetric stretching of -COO- (Masum et al., 2020), and indicative of the presence of carboxylic acid (Kusuma et al., 2021). This is supported by another study that proteins are known to contribute to FTIR spectra bands primarily found at 1,650 cm^{-1} to 1,665 cm^{-1} , 1,550 cm^{-1} , and 1,310 cm^{-1} to 1,200 cm^{-1} (Mabwa et al., 2021). The peak band at 1640 cm^{-1} is known as the protein amide groups (-CONH-) due to the carbonyl (C=O) stretching vibration of the peptide groups, which may indicate the occurrence of β -1, 4 linked glucose, and mannose of DAM. The glucose: mannose ratio of DAM has been reported to be 1:41 (Fu et al., 2004). The FTIR spectra in the region of 1,700-600 cm^{-1} provides information about main polysaccharides that present in complex polysaccharide mixtures, which mainly are dominated by C-O, C-C stretching vibrations, ring structures, and deformation vibrations of the CH₂ group (Huang et al., 2011). The FTIR spectra of the DAM at 1,150, 1,078, and 1,019 cm^{-1} may be assigned to C-O-C stretching modes from ether groups in the pyranose rings (Chua et al., 2012). In additions, the bands at 933 and 760 cm^{-1} were also confirmed as pyranose forms (Ma et al., 2017a). The spectrum at 847.95 cm^{-1} indicates the presence of β -1, 4 glucosidic and β -1, 4 mannosidic linkages characteristic of DAM that is assigned to C-O-C stretching. A research pointed out that a peak at 800 cm^{-1} indicates the presence of mannose from mucopolysaccharide of cassava roots (Charles et al., 2008), whereas mannose and glucose units of konjac glucomannan were assigned to β pyranose form (808.12 and 875.62 cm^{-1}) (Widjanarko et al., 2011). Furthermore, six bands are observed in the region between 1200 and 800 cm^{-1} , which is generally known as the "fingerprint" area for carbohydrates (Behbahani et al., 2017). Overall, the FTIR

results qualitatively suggest that DAM mainly containing polysaccharides as β -pyranose forms of glucose and mannose.

DAM powder has irregular shape with rough surface (Figure 5), which might be attributed by mechanical forces that broke the granular structures during the extraction process. Nevertheless, the morphology of DAM powder was similar to the morphology of konjac glucomannan (Yanuriati et al., 2017). The porosity of DAM provides an opportunity for rapid diffusion of other small molecules into DAM structures and forming gel. The porous surface might be attributed by the presence of polysaccharide and protein, which was confirmed by the FTIR results. However, starch granules might not be present in the DAM because the starch was removed by ethanol precipitation during extraction (Andrade et al., 2020).

DAM powder was quite white, which indicated by the whiteness index of 90.77. The whiteness index found in this study is similar to the value reported for purified konjac glucomannan, i.e., 91.34 (Yanuriati et al., 2017), but it is higher than the value of commercial konjac glucomannan, i.e., 88.03 (Tatirat and Charoenrein, 2011). Relatively white DAM granules may be attributed to the dissolution of pigment in ethanol, which was then discarded during filtration, and browning inactivation through steam blanching during extraction process of the mucilage. Colour of DAM powder is an important parameter that will affect its application in food products.

Dissolving DAM powder in bi-distilled water at 10% w/v resulted in a thick suspension with pH of 6.7. This was higher than pH of the freeze-dried yam mucilage, i.e., 6.30 (Tavares et al., 2011), and taro mucilage, i.e., 6.32 (Nagata et al., 2015). This result may be favourable for further applications of DAM powder in foods, which mostly require a neutral pH.

DAM powder had protein content of 0.37% w/w, which was similar to protein content of *D. opposita* mucilage powder, i.e., 0.21% (Ma et al., 2017c), but it was much lower than the protein content of taro mucilage, i.e., 3.18% (Nagata et al., 2015). The protein content can be related to emulsifying capacity of DAM, which has been reported for mucilage *D. opposita* mucilage (Ma et al., 2017a; Liu et al., 2019) and *D. rotundata* mucilage (Lozano et al., 2020). This capacity would involve ability of DAM to bind at oil-water interface. Therefore, WHC, OHC, and then emulsifying activity of the DAM were measured.

The WHC of DAM powder was 8.43 g water/g sample, which was much higher than that of mung bean mucilage powder (4.80 g water/g) (Song et al., 2019), tamarind seed mucilage powder (0.18-1.07 g water/g) (Alpizar-Reyes et al., 2017), and *Rosa roxburghii* Tratt fruit mucilage powder (0.25 g water/g) (Wang et al., 2018). The WHC represents the amount of water held and absorbed by one gram of dry polysaccharides. It is a sum of bound water, hydrodynamic water, and physically trapped water. WHC can be used to predict stability, texture, sensory, and rheology of many processed foods and interactions between components (Ghribi et al., 2015; Bayar et al., 2016). Based on the results, WHC of different mucilage powder varies, which may be attributed to different species, concentrations, types, content of proteins and polysaccharides. Particle size and density also affect WHC, with large particles but low density, meaning ample void in the particle, would trap significant amount of water (Boulos et al., 2000). OHC value of DAM powder was 5.08 g oil/g sample, which was much higher than *D. esculenta* mucilage powder, i.e., 1.57 g oil/g sample (Herlina, 2015) and *D. opposita* mucilage powder, i.e., 2.02 g oil/g sample (Lozano et al., 2018). The difference in OHC between mucilage of *Dioscorea* sp. may be attributed to chemical composition, ratio, and position of hydrophobic to hydrophilic groups present in particles, pore size, and analysis methods. High OHC may allow stabilization of high-fat food products and emulsions. Further, OHC plays an important role to retain flavour and increase mouthfeel of food products.

Emulsifying activity (EA) of DAM powder was 35.61%, which was similar as that of *D. rotundata* mucilage powder (33.07%) (Lozano et al., 2018) and taro mucilage powder (34.85%) (Andrade et al., 2020). EA can also be defined as emulsion stability because EA is calculated based on the ratio between the

remaining emulsion layer and the water phase layer after 30 min. Looking at the values, it seems that DAM, as well as other mucilages, poorly stabilized the emulsions because phase separation took place within a short period of time. *D. rotundata* mucilage was reported to give fat stability and retention of air bubbles in ice cream, considering its low emulsion stability (Lozano et al., 2022). Nevertheless, further study on physicochemical properties of DAM is necessary to unlock and elucidate further potency of DAM in food applications.

CONCLUSION

The RSM-CCD, followed by distance-optimality design, is an effective tool for the optimization of extraction conditions to get the highest yield of DAM from *D. alata* tuber. A second-order quadratic model was obtained to predict the extraction yield of DAM. The RSM-CCD exhibited a high value of R^2 (0.9959) and a non-significant lack of fit. The optimal extraction conditions to obtain the maximum DAM yield of 5.89% were acquired at an extraction temperature of 36.2°C, extraction time of 13.3 h, and centrifugal speed of 12,322×g which is very close to the experimental yield, i.e., 11.25%, under the same extraction conditions. The FTIR spectra showed that the DAM extracted under the optimum conditions mainly contained polysaccharides with the presence of glucomannan and protein, albeit with a low content, i.e., 0.37%. DAM powder seemed to be superior for its WHC and OHC, but its emulsifying activity was low.

ACKNOWLEDGEMENTS

The research was financially supported by Beasiswa Unggulan Dosen Indonesia Dalam Negeri (BUDIDN) Program, Ministry of Education and Culture of the Republic of Indonesia; and The Indonesia Endowment Fund for Education (LPDP), Ministry of Finance of the Republic of Indonesia.

AUTHOR CONTRIBUTIONS

Dewi Fortuna conceived and designed an analysis of DAM extraction, performed statistical analyses, interpreted results, and wrote the paper. Emmy Darmawati performed statistical analyses and results with the first author. Titi Candra Sunarti contributed to the analysis design and corrected the final paper. Sutrisno supervised the experimental data. Nanik Purwanti initiated this research and directed the entire experimental study. She also supervised the article redaction and interpretation of the results and edited the manuscript with the first author. Siti Mariana Widayanti and Nancy Dewi Yuliana corrected the final paper.

CONFLICT OF INTEREST

The authors declare that they hold no competing interests.

REFERENCES

- Alpizar-Reyes, E., Carrillo-Navas, H., Gallardo-Rivera, R., Varela-Guerrero, V., Alvarez-Ramirez, J., and Pérez-Alonso, C. 2017. Functional properties and physicochemical characteristics of tamarind (*Tamarindus indica* L.) seed mucilage powder as a novel hydrocolloid. *Journal of Food Engineering*. 209: 68–75.
- Alves, R.M., Grossmann, M.V., Ferrero, C., Zaritzky, N.E., Martino, M.N., and Sierakoski, M.R. 2002. Chemical and functional characterization of products obtained from yam tubers. *Starch/Staerke*. 54: 476–481.
- Andrade, L.A., de Oliveira Silva, D.A., Nunes, C.A., and Pereira, J. 2020. Experimental techniques for the extraction of taro mucilage with enhanced emulsifier properties using chemical characterization. *Food Chemistry*. 327: 127095.
- Bayar, N., Kriaa, M., and Kammoun, R. 2016. Extraction and characterization of three polysaccharides extracted from *Opuntia ficus-indica* cladodes. *International Journal of Biological Macromolecules*. 92: 441–450.
- Behbahani, B.A., Yazdi, F.T., Shahidi, F., Hesarinejad, M.A., Mortazavi, S.A., and Mohebbi, M. 2017. *Plantago* major seed mucilage: Optimization of extraction and some physicochemical and rheological aspects. *Carbohydrate Polymers*. 155: 68–77.
- Berk, Z. 2018. *Food Process Engineering and Technology* (3rd Ed.). Academic Press. London
- Boulos, N.N., Greenfield, H. and Wills, R.B.H. 2000. Water holding capacity of selected soluble and insoluble dietary fibre. *International Journal of Food Properties*. 3(2): 217–231.
- Bukhari, S.N.A., Ali, A., Hussain, M.A., Tayyab, M., Alotaibi, N. F., Elsherif, M. A., Junaid, K., and Ejaz, H. 2022. Extraction optimization of mucilage from seeds of *Mimosa pudica* by response surface methodology. *Polymers*. 14(9): 1–16.
- Chien, W.J., Saputri, D.S., Yanti, S., and Agrawal, D.C. 2022. Response surface methodology for simple non-acid ultrasonic-assisted extraction of pectin from Taiwan's citrus depressa h. peels. *Chiang Mai University Journal of Natural Sciences*. 21(4): e2022062.
- Chan, C.H., Yusoff, R., and Ngoh, G.C. 2014. Modeling and kinetics study of conventional and assisted batch solvent extraction. *Chemical Engineering Research and Design*. 92(6): 1169–1186.
- Charles, A. L., Huang, T.C., and Chang, Y.H. 2008. Structural analysis and characterization of a mucopolysaccharide isolated from roots of cassava (*Manihot esculenta* Crantz L.). *Food Hydrocolloids*. 22: 184–191.
- Chua, M., Chan, K., Hocking, T.J., Williams, P.A., Perry, C.J., and Baldwin, T.C. 2012. Methodologies for the extraction and analysis of konjac glucomannan from corms of *Amorphophallus konjac* K. Koch. *Carbohydrate Polymers*. 87: 2202–2210.
- Fortuna, D., Mardjan, S.S., Sunarti, T.C., Darmawati, E., Widayati, S.M., and Purwanti, N. 2020. Extraction and characteristic of *Dioscorea alata* mucilage. *IOP Conference Series: Earth and Environmental Science*. 542(1): 12016.
- Fu, Y.C., Chen, S. and Lai, Y.J. 2004. Centrifugation and foam fractionation effect on mucilage recovery from *Dioscorea* (yam) tuber. *Journal of Food Science*. 69(9): 509–514.
- Garcia-Vaquero, M., Rajauria, G., and Tiwari, B. 2020. Chapter 7 - Conventional extraction techniques: Solvent extraction (pp. 171–189). In M. D. Torres, S. Kraan and H. Dominguez (Eds). *Advances in Green and Sustainable Chemistry, Sustainable Seaweed Technologies*. Elsevier Inc.
- Garedew, B., Haile, B., and Ayiza, A. 2017. Distribution, diversity and potential production of yams (*Dioscorea* spp.) in Sheko District, Southwest Ethiopia. *American Journal of Life Sciences*. 5(3): 86–92.

- Ghribi, A.M., Sila, A., Gafsi, I.M., Blecker, C., Danthine, S., Attia, H., Bougatef, A., and Besbes, S. 2015. Structural, functional and ACE inhibitory properties of water-soluble polysaccharides from Chickpea flours. *International Journal of Biological Macromolecules*. 75: 276–282.
- Han, Y.L., Gao, J., Yin, Y.Y., Jin, Z.Y., Xu, X.M., and Chen, H.Q. 2016. Extraction optimization by response surface methodology of mucilage polysaccharide from the peel of *Opuntia dillenii* haw. fruits and their physicochemical properties. *Carbohydrate Polymers*. 151: 381–391.
- Herlina. 2015. Deproteinase effect of hydrocolloid flour made of "Gembili tuber " (*Dioscorea esculenta* L.) on chemical and technical functional properties. *International Journal on Advanced Science, Engineering and Information Technology*. 5(4): 298–302.
- Hong-rui, L., Shu-Lin, Y., Yun-chao, C., and Li-qiang, Z. 2010. Optimization of extraction process of *rhizoma Dioscoreae* polysaccharide and determination of its antioxidant activity. *Medicinal Plant*. 1(12): 29–32.
- Huang, Z., Liang, Z., Li, G., and Hong, H. 2011. Response surface methodology to extraction of *Dioscoreae* polysaccharides and the effects on rat's bone quality. *Carbohydrate Polymer*. 83: 32–37.
- Huang R., Xie, J., Yu, Y., and Shen, M. 2020. Recent progress in the research of yam mucilage polysaccharides: Isolation, structure and bioactivities. *International Journal of Biological Macromolecules*. 155: 1262–1269.
- Hui, H., Jin, H., Li, X., Yang, X., Cui, H., Xin, A., Zhao, R., and Qin, B. 2019. Purification, characterization and antioxidant activities of a polysaccharide from the roots of *Lilium davidii* var. unicolor cotton. *International Journal of Biological Macromolecules*. 135: 1208–1216.
- Jongjareonrak, A., Srikok, K., Leksawasdi, N., and Andreotti, C. 2015. Extraction and functional properties of protein from de-oiled rice bran. *Chiang Mai University Journal of Natural Sciences*. 14(2): 163–174.
- Kusuma, H.S., Amenaghawon, A.N., Darmokoesoemo, H., Neolaka, Y.A.B., Widyaningrum, B.A., Anyalewechi, C.L., and Orukpe, P.I. 2021. Evaluation of extract of *Ipomoea batatas* leaves as a green coagulant–flocculant for turbid water treatment: Parametric modelling and optimization using response surface methodology and artificial neural networks. *Environmental Technology and Innovation*. 24: 102005.
- Kusuma, H.S., and Mahfud, M. 2017. The extraction of essential oils from patchouli leaves (*Pogostemon cablin benth*) using a microwave air-hydrodistillation method as a new green technique. *RSC Advances*. 7(3) : 1336–1347.
- Kusuma, H.S., Sudrajat, R.G.M., Susanto, D.F., Gala, S., and Mahfud, M. 2015. Response surface methodology (RSM) modeling of microwave-assisted extraction of natural dye from *Swietenia mahagony*: A comparison between Box-Behnken and central composite design method. *International Conference of Chemical and Material Engineering*. 1699: 050009.
- Lebot, V., Malapa, R., Abraham, K., Molisale, T., Kien, N. Van, Gueye, B., and Waki, J. 2018. Secondary metabolites content may clarify the traditional selection process of the greater yam cultivars (*Dioscorea alata* L.). *Genetic Resources and Crop Evolution*. 65(6): 1699–1709.
- Leyva-Jiménez, F. J., Fernández-Ochoa, Á., Cádiz-Gurrea, M. de la L., Lozano-Sánchez, J., Oliver-Simancas, R., Alañón, M. E., Castangia, I., Segura-Carretero, A., and Arráez-Román, D. 2022. Application of response surface methodologies to optimize high-added value products developments: cosmetic formulations as an example. *Antioxidants*. 11(8): 1–23.
- Li, Q., Zhang, C.R., Dissanayake, A.A., Gao, Q., and Nair, M.G. 2016. *Phenanthrenes* in chinese yam peel exhibit antiinflammatory activity, as shown by strong in vitro cyclooxygenase enzyme inhibition. *Natural Product Communications*. 11(9): 1313–1316.
- Li, Q., Zhang, L., Ye, Y., and Gao, Q. 2015. Effect of salts on the gelatinization process of Chinese yam (*Dioscorea opposita*) starch with digital image analysis method. *Food Hydrocolloids*. 51: 468–475.

- Li, X., Ren, Z., Wang, R., Liu, L., Zhang, J., Ma, F., Khan, M.Z.H., Zhao, D., dan Liu, X. 2021. Characterization and antibacterial activity of edible films based on carboxymethyl cellulose, *Disocorea opposita* mucilage, glycerol and ZnO nanoparticles. *Food Chemistry*. 349: 129208.
- Liu, X. X., Yan, Y.Y., Liu, H.M., De Wang, X., and Qin, G.Y. 2019. Emulsifying and structural properties of polysaccharides extracted from chinese yam by an enzyme-assisted method. *LWT - Food Science Technology*. 111(May): 242–251.
- Liu, Y., Li, H., Fan, Y., Man, S., Liu, Z., Gao, W., and Wang, T. 2016. Antioxidant and antitumor activities of the extracts from Chinese yam (*Dioscorea opposita* Thunb.) flesh and peel and the effective compounds. *Journal of Food Science*. 81(6): H1553–H1564.
- Lozano, E.J., Andrade, R.D., and Salcedo, J.G. 2018. Functional and rheological properties of yam (*Dioscorea rotundata*) mucilage. *Advance Journal of Food Science and Technology*. 15(SPL): 134–142.
- Lozano, E., Salcedo, J., and Andrade, R. 2020. Evaluation of yam (*Dioscorea rotundata*) mucilage as a stabilizer in the production of mango nectar. *Heliyon*. 6: e04359.
- Lozano, E., Padilla, K., Salcedo, J., Arrieta, A., and Andrade, R. 2020. Effects of yam (*Dioscorea rotundata*) mucilage on the physical, rheological and stability characteristics of ice cream. *Polymer*. 14(15): 3142.
- Luo, D. 2012. Optimization of total polysaccharide extraction from *Dioscorea nipponica* Makino using response surface methodology and uniform design. *Carbohydrate. Polymers*. 90(1): 284–288.
- Ma, F., Wang, R., Li, X., Kang, W., Bell, A.E., Zhao, D., Liu, X., and Chen, W. 2020. Physical properties of mucilage polysaccharides from *Dioscorea opposita* Thunb. *Food Chemistry*. 311: 126039.
- Ma, F., Zhang, Y., Yao, Y., Wen, Y., Hu, W., Zhang, J., Liu, X., Bell, A.E., and Tikkanen-Kaukanen, C. 2017a. Chemical components and emulsification properties of mucilage from *Dioscorea opposita* Thunb. *Food Chemistry*. 228: 315–322.
- Ma, F., Zhang, Y., Liu, N., Zhang, J., Tan, G., Kannan, B., Liu, X., and Bell, A.E. 2017b. Rheological properties of polysaccharides from *Dioscorea opposita* Thunb. *Food Chemistry*. 227: 64–72.
- Ma, F., Zhang, Y., Wen, Y., Yao, Y., Zhu, J., Liu, X., Bell, A., and Tikkanen-kaukanen, C. 2017c. Emulsification properties of polysaccharides from *Dioscorea opposita*. *Food Chemistry*. 221: 919–925.
- Mabwa, D., Gajjar, K., Furniss, D., Schiemer, R., Crane, R., Fallaize, C., Martin-Hirsch, P.L., Martin, F.L., Kypraios, T., Seddon, A.B., and Phang, S. 2021. Mid-infrared spectral classification of endometrial cancer compared to benign controls in serum or plasma samples. *Analyst*. 146(18): 5631–5642.
- Maneenoon, K., Sirirugsa, P., and Sridith, K. 2008. Ethnobotany of *Dioscorea* L. (*Dioscoreaceae*), a major food plant of the Sakai Tribe at Banthad Range, Peninsular Thailand. *Ethnobotany Research and Applications*. 6: 385–394.
- Masum, A.Al., Pal, K., Saha, I., Ghosh, D., Roy, S., Chowdhury, S.G., Islam, M.M., and Karmakar, P. 2020. Facile synthesis of antibiotic encapsulated biopolymeric okra mucilage nanoparticles: Molecular docking, *in vitro* stability and functional evaluation. *Advances in Natural Sciences: Nanoscience and Nanotechnology*. 11(2): 025020.
- Misaki, A., Ito, T., and Harada, T. 1972. Constitutional Studies on the Mucilage of "Yamanoimo," *Dioscorea batatas* Decne, forma Tsukune. *Agricultural and Biological Chemistry*. 36(5): 761–771.
- Mistry, A.H., Schmidt, S.J., Eckhoff, S.R., and Sutherland, J.W. 1992. Alkali extraction of starch from corn flour. *Starch/Stärke*. 44(8): 284–288.
- Montgomery, D.C. 2013. Design and analysis of experiments. John Wiley & Sons
- Nagai, T., Suzuki, N., Kai, N., and Tanoue, Y. 2014. Functional properties of autolysate and enzymatic hydrolysates from yam tsukuneimo (*Dioscorea opposita* Thunb.) tuber mucilage tororo: Antioxidative activity and antihypertensive activity. *Journal of Food Science Technology*. 51(12): 3838–3845.

- Nagata, C.L.P., Andrade, L.A., and Pereira, J. 2015. Optimization of taro mucilage and fat levels in sliced breads. *Journal of Food Science Technology*. 52(9): 5890–5897.
- Nandiyanto, A.B.D., Oktiani, R., and Ragadhita, R. 2019. How to read and interpret FTIR spectroscopy of organic material. *Indonesian Journal of Food Science Technology*. 4(1): 97–118.
- Narkhede, A., Gill, J., Thakur, K., Singh, D., Singh, E., Kulkarni, O., Harsulkar, A., and Jagtap, S. 2013. Total polyphenolic content and free radical quenching potential of *Dioscorea alata* L. tubers. *International Journal of Pharmacy and Pharmaceutical Sciences*, 5(3): 3–6.
- Nawrocka, A., Krekora, M., Niewiadomski, Z., and Mi, A. 2018. FTIR studies of gluten matrix dehydration after fibre polysaccharide addition. *Food Chemistry*. 252: 198–206.
- Saepang, K., Pitaksuteepong, T., Buranrat, B., and Boontha, S. 2024. Optimization of HPMC-based oral fast dissolving film of cetirizine dihydrochloride. *Natural and Life Sciences Communications*. 23(1): e2024007.
- Song, Q., Jiang, L., Yang, X., Huang, L., Yu, Y., Yu, Q., Chen, Y., and Xie, J. 2019. Physicochemical and functional properties of a water-soluble polysaccharide extracted from mung bean (*Vigna radiate* L.) and its antioxidant activity. *International Journal of Biological Macromolecules*. 138: 874–880.
- Stamenković, O.S., Kostić, M.D., and Dragana, B. 2018. Comparison of Box-Behnken, face central composite and full factorial designs in optimization of hempseed oil extraction by n-hexane: A case study. *Periodica Polytechnica Chemical Engineering*. 62(3): 359–367.
- Suzuki, T., Ohsugi, Y., Yoshie, Y., Shirai, T., and Hirano, T. 1996. Dietary fiber content, water-holding capacity and binding capacity of seaweeds. *Fisheries Science*. 62(3): 454–461.
- Tatirat, O. and Charoenrein, S. 2011. Physicochemical properties of konjac glucomannan extracted from konjac flour by a simple centrifugation process. *LWT - Food Science and Technology*. 44(10): 2059–2063.
- Tavares, S. A., Pereira, J., Guerreiro, M.C., Pimenta, C.J., Pereira, L., and Missagia, S.V. 2011. Physical and chemical characteristics of the mucilage of lyophilized yam. *Ciência e Agrotecnologia*. 35(5): 973–979.
- Thaisungnoen, K., Umar, M., Singh, M., and Anal, A.K. 2024. Ultrasonic-assisted extraction of bioactive extract from Napier grass (*Pennisetum purpureum*), evaluation of its bioactivity, antimutagenicity and cytotoxicity. *Natural and Life Sciences Communications*. 23(1): e2024014.
- Tosif, M. M., Najda, A., Klepacka, J., Bains, A., Chawla, P., Kumar, A., Sharma, M., Sridhar, K., Gautam, S.P., and Kaushik, R. 2022. A concise review on taro mucilage: extraction techniques, chemical composition, characterization, applications, and health attributes. *Polymers*. 14: 1163.
- Waghmare, R., Preethi, R., Moses, J.A., and Anandharamakrishnan, C. 2022. Mucilages: sources, extraction methods, and characteristics for their use as encapsulation agents. *Critical Reviews in Food Science and Nutrition*. 62(15): 4186–4207.
- Wang, L., Zhang, B., Xiao, J., Huang, Q., Li, C., and Fu, X. 2018. Physicochemical, functional, and biological properties of water-soluble polysaccharides from *Rosa roxburghii* Tratt fruit. *Food Chemistry*. 249: 127–135.
- Wang, R., Li, X., Liu, L., Chen, W., Bai, J., Ma, F., Liu, X., and Kang, W. 2020. Preparation and characterization of edible films composed of *Dioscorea opposita* Thunb. mucilage and starch. *Polymer Testing*. 90(106708): 1–8.
- Widjanarko, S.B., Nugroho, A., and Estiasih, T. 2011. Functional interaction components of protein isolates and glucomannan in food bars by FTIR and SEM studies. *African Journal of Food Science*. 5(1): 12–21.
- Yanuriati, A., Marseno, D.W., Rochmadi and Harmayani, E. 2017. Characteristics of glucomannan isolated from fresh tuber of porang (*Amorphophallus muelleri* Blume). *Carbohydrate Polymers*. 156: 56–63.

- Yasumatsu, K., Sawada, K., Moritaka, S., Misaki, M., Toda, J., Wada, T., and Ishii, K. 1972. Whipping and emulsifying properties of soybean products. *Journal of Agricultural and Biological Chemistry*. 36(5): 719–727.
- Yuan-yuan, W., Lan-Shu, X., Wei, F., Yong-Wei, G., and Zhao-Lin, L. 2015. Optimization of extraction process for investigation of polysaccharides yield and activity from Chinese yam. *Journal of Food Safety and Quality*. 6(6): 1980–1986.
- Zhang, L., and Wang, M. 2017. Optimization of deep eutectic solvent-based ultrasound-assisted extraction of polysaccharides from *Dioscorea opposita* Thunb. *International Journal of Biological Macromolecules*. 95: 675–681.
- Zhang, Z., Wang, X., Liu, C., and Li, J. 2016. The degradation, antioxidant and antimutagenic activity of the mucilage polysaccharide from *Dioscorea opposita*. *Carbohydrate Polymers*. 150: 227–231.
- Zhao, C., Li, X., Miao, J., Jing, S., Li, X., Huang, L., and Gao, W. 2017. The effect of different extraction techniques on property and bioactivity of polysaccharides from *Dioscorea hemsleyi*. *International Journal of Biological Macromolecules*. 102: 847–856.
- Zhi, F., Yang, T. Le, Wang, Q., Jiang, B., Wang, Z. P., Zhang, J., and Chen, Y. Z. 2019. Isolation, structure and activity of a novel water-soluble polysaccharide from *Dioscorea opposita* Thunb. *International Journal of Biological Macromolecules*. 133: 1201–1209.

OPEN access freely available online

Natural and Life Sciences Communications

Chiang Mai University, Thailand. <https://cmuj.cmu.ac.th>